



## Get Clarity On Generics

Cost-Effective CT & MRI Contrast Agents



FRESENIUS  
KABI

WATCH VIDEO

# AJNR

## Measurement of cerebral blood volume via the relaxing effect of low-dose gadopentetate dimeglumine during bolus transit.

T Hackländer, J R Reichenbach, M Hofer and U Mödder

*AJNR Am J Neuroradiol* 1996, 17 (5) 821-830

<http://www.ajnr.org/content/17/5/821>

This information is current as  
of August 19, 2025.

# Measurement of Cerebral Blood Volume via the Relaxing Effect of Low-Dose Gadopentetate Dimeglumine during Bolus Transit

Thomas Hackländer, Jürgen R. Reichenbach, Matthias Hofer, and Ulrich Mödder

**PURPOSE:** To quantify regional cerebral blood volume (rCBV) on the basis of the enhancement of blood proton relaxation rates after intravenous administration of gadopentetate dimeglumine. **METHODS:** A series of sequential MR images of one section was recorded during bolus transit with a standard fast low-angle shot sequence. The signal-intensity curves were converted into corresponding concentration-time curves from which rCBV images were calculated. **RESULTS:** The functional parameter images of rCBV were calculated pixel-by-pixel for two patients who had received a 1-second bolus injection of 1 mmol of gadopentetate dimeglumine. In a larger series of 62 patients, a mean blood volume of  $4.6 \pm 1.6$  vol% was determined for normal brain tissue. **CONCLUSIONS:** The relaxing effect of a contrast agent can be used to determine blood volume quantitatively. The results are in agreement with those obtained by nuclear medicine techniques. The proposed method requires no special hardware, and can thus be implemented on clinical MR scanners.

**Index terms:** Blood, volume; Brain, magnetic resonance; Magnetic resonance, flow studies

*AJNR Am J Neuroradiol* 17:821-830, May 1996

Recently, there has been growing interest in the assessment of physiological parameters on brain perfusion that provide more information than purely morphologic diagnosis. For instance, it is possible to determine the extent of vital tumors by evaluating changes in regional blood volume (1) even without apparent damage to the blood-brain barrier. In a similar way, the extent of an infarct can be assessed and its response to therapy can be followed (2, 3).

All methods presently used for determining cerebral blood volume (CBV) or flow are based on the dilution of an indicator that reaches the blood vessels of the organ. The concentration of the indicator is registered in a vein through direct extraction or through external measure-

ment as a function of time. As long as the indicator remains inside the vascular compartment it does not matter whether it is a dye, a radioactive substance, or a paramagnetic relaxation enhancer. It is possible to infer the blood volume and flow from the amount of agent administered as well as from the time-dependence of its concentration leaving the organ. The standard technique used today is positron emission tomography (PET), a technique that is available only at a few medical centers.

Several research groups have investigated possibilities for measuring regional cerebral blood volume (rCBV) by nuclear magnetic resonance (MR) imaging (4, 5). They exploited the susceptibility effect of gadopentetate dimeglumine after a bolus injection using the echo-planar technique for imaging. Recent studies show that this effect can also be measured by using conventional gradient-echo sequences (6, 7). The temporal resolution that can be achieved with the latter technique is, however, quite poor and typically requires acquisition times of more than 2 seconds per image for a  $64 \times 256$  matrix (8). Since the mean transit time of the bolus through the brain is about 10

---

Received April 13, 1995; accepted after revision September 7.

Supported in part by the Deutsche Forschungsgemeinschaft (SFB 194-A9).

From the Departments of Diagnostic Radiology (T.H., J.R.R., U.M.) and Anatomy II (M.H.), Heinrich-Heine-Universität, Düsseldorf, Germany.

Address reprint requests to Thomas Hackländer, Department of Diagnostic Radiology, Heinrich-Heine-Universität, Moorenstraße 5, D-400225 Düsseldorf, Germany.

*AJNR* 17:821-830, May 1996 0195-6108/96/1705-0821

© American Society of Neuroradiology

to 15 seconds, there are only a few data points available for tracking the passage of the bolus. To overcome this limitation and to achieve a sufficient spatial and temporal resolution, even with conventional scanners, Dean et al (9) proposed using the relaxing effect of paramagnetic contrast agents to determine the concentration as a function of time. Using the work of Dean et al as a basis for our study, we extended and refined this method. The results for CBV obtained in a typical sample population as well as from case studies show the advantages of the method and its applicability to routine clinical examinations.

## Materials and Methods

### Mathematical Model

The mathematical model of Zierler (10, 11) for determining blood volume or flow is based on a black-box system with one inlet and one outlet. The internal structure of the system is not taken into consideration. Each particle of a rapidly injected amount  $Q$  of tracer requires a certain time before it reappears at the outlet. This time is denoted as transit time and depends on the particular path (trajectory) the particle has taken through the system. Consequently, the concentration  $c_{out}(t)$  of the tracer at the outlet can be interpreted in terms of a probability density function  $h(t)$  for all possible transit times of tracer particles (12):

$$1) \quad c_{out}(t) = \frac{Q}{F} \cdot h(t)$$

where  $F$  denotes the volume flow in units of milliliters per second. Equation 1 is based on the assumption that it is possible to determine the indicator concentration in the draining vessel. If MR tomography is used, this assumption is generally not valid. Rather, each voxel is regarded as a small, homogeneous, single system. Instead of measuring the concentration at the outlet, the fraction  $R(t)$  of the initial bolus, which remains in the system at time  $t$ , is determined (13). The residue function  $R(t)$  is defined as follows:

$$2) \quad R(t) = 1 - \int_0^t h(t') dt'$$

Equation 2 assumes that the entire bolus enters the system at  $t = 0$ ; that is, the injection must ideally be infinitely brief. With Equation 2, one can express the blood volume  $CBV_{vox}$  in a voxel of tissue (10), where  $F_{vox}$  denotes the flow in the voxel (in milliliters per second):

$$3) \quad CBV_{vox} = F_{vox} \cdot \int_0^\infty t \cdot h(t) dt = F_{vox} \cdot \int_0^\infty R(t) dt$$

The relationship between  $R(t)$  and directly measurable

quantities can be established in the following way (14):

$$4) \quad q(t) = q(0) \cdot R(t)$$

where the amount of indicator  $q(0)$  entering the voxel at time  $t = 0$  represents the fraction of the total injected amount  $Q$ , which is proportional to the ratio of the volume flows within the voxel,  $F_{vox}$ , and the major artery supplying the voxel,  $F_a$ , respectively.

$$5) \quad q(t) = \frac{Q \cdot F_{vox}}{F_a} \cdot R(t)$$

It is assumed that all voxels are supplied by the same artery, which in our case is the aorta. Consequently,  $F_a$  denotes the flow in the aorta.

Using a radioactive tracer as an indicator, we can determine the amount  $q(t)$  directly by measuring the decay rate. This is different in MR imaging, where the measured signal in each voxel is a function of proton density, susceptibility, and relaxation times of the tissue. In the presence of a paramagnetic agent, part of these physical properties are changed. The concentration  $c_{vox}$  of the indicator in a voxel can be determined from the measured signal  $S$ , assuming that the signal is a monotone function of the indicator concentration in the blood.

Since each voxel is assumed to be homogeneous, Equation 5 can be transformed into an equation for the concentration by dividing both sides by the known voxel volume  $V_{vox}$

$$6) \quad c_{vox}(t) = \frac{Q \cdot F_{vox}}{V_{vox} \cdot F_a} \cdot R(t)$$

Inserting Equation 6 into Equation 3, it follows that the integral over the concentration-time curve measured within one voxel is proportional to the rCBV:

$$7) \quad CBV_{vox} = \frac{V_{vox} \cdot F_a}{Q} \cdot \int_0^\infty c_{vox}(t) dt$$

Equation 7 also holds true for a "real" bolus under the assumption that the mean temporal width of the initial bolus is shorter than the mean transit time through the system (13). To determine the unknown prefactor

$$8) \quad \frac{V_{vox} \cdot F_a}{Q}$$

a voxel in the imaged section is selected that lies entirely within a draining vessel (eg, in the sagittal sinus). For this volume we can write, using Equation 7,

$$9a) \quad CBV_{vessel} = V_{vox} = \frac{V_{vox} \cdot F_a}{Q} \cdot \int_0^\infty c_{vessel}(t) dt$$

hence,

$$9b) \quad \frac{F_a}{Q} = \frac{1}{\int_0^\infty c_{vessel}(t) dt}$$

Inserting Equation 9 into Equation 7 gives the fractional blood volume of an arbitrary voxel within brain tissue:

$$10a) \quad rCBV = \frac{CBV_{vox}}{V_{vox}} = \frac{\int_0^{\infty} c_{vox}(t) dt}{\int_0^{\infty} c_{vessel}(t) dt}$$

or the rCBV expressed as a percentage:

$$10b) \quad rCBV\% = \frac{CBV_{vox}}{V_{vox}} \cdot 100$$

### Contrast Agent

The contrast agent gadopentetate dimeglumine has no direct influence on the MR signal, but it acts indirectly by decreasing the relaxation times of the surrounding nuclear spins (15, 16). This effect is proportional to the gadolinium concentration and is expressed numerically in terms of a relaxivity  $R$  for T1 and T2. We have measured the following relaxivities for gadopentetate dimeglumine in human blood serum at 38°C in a magnetic field of 1.5 T:

$$R1 = 3.7 \text{ [L/mmol}\cdot\text{s]}; R2 = 4.9 \text{ [L/mmol}\cdot\text{s]}$$

Since the measurements were performed with a whole-body scanner, the relative errors for the actual numbers were estimated to range from 10% to 15%.

After intravenous injection, the agent is distributed in the plasma without any incorporation of molecules into erythrocytes (17). Thus, plasma volume must be considered as the *primary distribution volume*. Owing to the rapid exchange of water molecules (half-time of about 10 microseconds) between intraplasmic and intraerythrocytic compartments, all protons in the intravascular compartment are involved in the relaxation processes during the acquisition time of an image. On the one hand, the entire intravascular compartment must be considered as the *effective distribution volume*. On the other hand, exchange with the extravascular compartment is negligible in the first approximation, as the corresponding time constant is only about 500 milliseconds.

Because of its high molecular weight and hydrophilic nature, the contrast agent does not pass the blood-brain barrier under normal physiological conditions. In other body tissues and in brain tumors, however, it does leave the intravascular compartment but the molecules always remain in the extracellular spaces (18). In the case of brain tumors in which there is a disturbed blood-brain barrier, the kinetics of contrast agent uptake were studied by Gowland et al (18). For passive transport from the intravascular to the extracellular compartment, these authors reported a time of 120 to 900 seconds, depending on the type of tumor, until a maximum concentration within the tissue is reached. Assuming an exponential uptake of contrast agent and assuming that the reported values are reached within three half-times (corresponding to 95% of

the maximum value), diffusion times between 30 and 200 seconds are obtained for the passage of the agent into the tumor. With a mean bolus transit time of approximately 10 seconds through the brain, gadopentetate dimeglumine can almost be regarded to be an intravascular contrast agent, even in cases of a disturbed blood-brain barrier.

### Measuring Sequence

It is important to use a high imaging rate to obtain functional parameter images during the first passage of a bolus of gadopentetate dimeglumine. With echo-planar imaging, an acquisition time of less than 100 milliseconds per image can be achieved (19, 20). Unfortunately, this method requires a special gradient system not routinely available on most clinical scanners. Furthermore, the generated images are inherently T2\* weighted, which complicates the investigation of T1 relaxation phenomena.

Alternatively, the fast low-angle shot sequence allows imaging times of about 300 to 900 milliseconds per image with standard whole-body scanners (21). Owing to the short repetition times, TR, the spin system does not necessarily reach magnetic equilibrium within the acquisition of one image (22). Only after continuously acquiring images of one particular section does a steady state evolve, for which the signal can be written as (23)

$$11) \quad S_{\infty} f = \frac{(1-E1) \cdot \sin \alpha}{(1-E1 \cdot \cos \alpha) + E2 \cdot (E1 - \cos \alpha)} \cdot E3$$

with

$$\begin{aligned} 12) \quad E1 &= \exp(-TR \cdot (1/T1 + c \cdot R1)) \\ E2 &= \exp(-TR \cdot (1/T2^* + c \cdot R2)) \\ E3 &= \exp(-TE \cdot (1/T2^* + c \cdot R2)) \end{aligned}$$

where TR denotes the repetition time, TE the echo time,  $\alpha$  the flip angle, T1 and T2\* the initial spin-lattice and effective spin-spin relaxation time, respectively. The symbol  $c$  denotes the concentration, and R1 and R2 the corresponding relaxivities of the agent. Strictly speaking, Equation 11 describes the signal obtained from a refocused fast low-angle shot sequence in which the effect of incrementing the phase-encoding gradient has been canceled by applying a reverse gradient in each cycle between the collection of data and the onset of the next radio frequency pulse. By contrast, the original fast low-angle shot sequence is a spoiling sequence, in which transverse magnetization is destroyed between cycles. To save time, neither a spoiling nor a refocusing gradient was applied in the present sequence. Thus, Equation 11 represents only an approximation, which, however, describes the signal-concentration relationship for low concentrations up to 2 mmol very well. This can be seen in Figure 1, in which we have plotted signal versus concentration of gadopentetate dimeglumine in human serum at 38°C.

Mobile structures, particularly flowing blood, do not reach a steady state. Flowing blood is therefore imaged

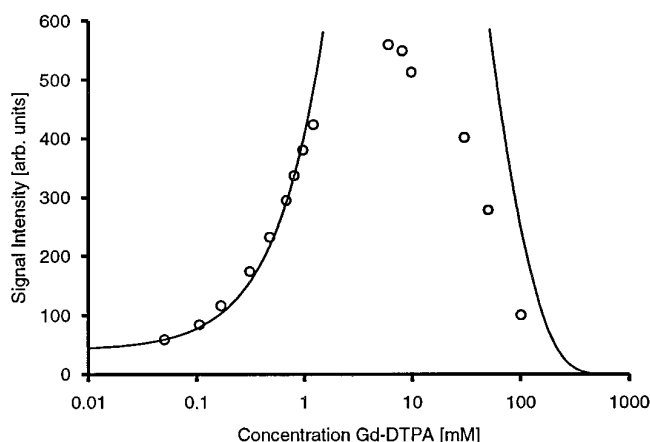


Fig 1. Results of a dilution series of gadopentetate dimeglumine (Gd-DTPA) in human serum at 38°C. The signal intensity is plotted against the concentration (in millimoles) on a logarithmic scale. The dots represent the experimental values, the solid line shows the theoretically expected signal intensity using Equation 11 with the same sequence parameters used in the in vivo studies.

with a very high signal intensity. Specially prepared pulses before the actual fast low-angle shot sequence is initiated (24) can suppress these signal enhancements. Suppression is most easily accomplished with a nonselective 180° pulse that inverts all the spins within the volume being imaged. If the time interval between successive images is distinctly shorter than the T1 relaxation of the brain tissue, the influence of the preparation pulse is no longer specific for a particular tissue.

In large venous vessels, such as the sagittal sinus, the velocity of blood is about 20 cm/s which leads to a strong signal enhancement even with an inversion pulse. These effects were taken into account during data evaluation and corrected for with an empirically determined factor of 0.9 (25).

Figure 1 shows that there is a well-defined relationship between signal intensity and gadolinium concentration for values below a critical level corresponding to the maximum signal. By choosing the correct amount and time span for injecting gadopentetate dimeglumine, one can ensure that this critical level is not exceeded (26). In our investigations, the highest bolus concentrations measured in the internal carotid artery were below 2 mmol.

The measured nuclear spin signal  $S(t)$  consists of two contributions from brain tissue,  $S_{tissue}$ , and from vessels embedded in it,  $S_{vasc}$ , respectively. Since only the vascular component is influenced by the contrast bolus, the signal  $S(t)$  can be written as

$$13) \quad S(t) = S_{tissue} + S_{vasc}(c(t))$$

Performing a native measurement before the bolus arrives allows the signal changes to be determined:

$$14) \quad \Delta S(t) = S_{vasc}(c(t)) - S_{vasc}(c(t=0))$$

Equation 14 can be rewritten as

$$15) \quad \Delta S(c(t)) = A \cdot \rho \cdot [f_{vasc}(c(t)) - f_{vasc}(c(t=0))]$$

where  $A$  denotes a proportionality constant that is dependent on the actual instrumental settings,  $\rho$  is the proton density, and  $f$  is given by Equation 11.

We assume that at time  $t = 0$  no contrast agent is present in the particular voxel under consideration. Although  $\Delta S(c(t))$  is the measurable quantity, we are actually interested in obtaining concentration values  $c(t)$ . This can be achieved by applying the inverse function  $C(\Delta S)$ , which allows  $c$  to be calculated for a given  $\Delta S$ . Formally,

$$16) \quad c(t) = C\{\Delta S(c(t))\}$$

Equation 15 still contains the constant  $A$ , which has to be determined separately for each examination. In principle, it is possible to use external or internal standards for reference measurements. Although it is preferable to calibrate the measurement with an external reference phantom with well known physical properties, there is, from a practical point of view, one important advantage in using an internal standard. Frequently, during a typical clinical examination, an rCBV measurement is appropriate or necessary. Use of an internal standard allows for this option without having to move the patient in order to place the external reference near the head.

For that practical reason we defined a sufficiently large region of interest within white matter on axial images in order to obtain a reference region with known relaxation properties. Since the relaxation times for white matter are well known, we can calculate  $f_{ref}$  from Equation 11 and take the signal intensity  $S_{ref}$  directly from the measured data. Thus,  $A$  can be determined:

$$17) \quad A = \frac{S_{ref}}{\rho_{ref} \cdot f_{ref}}$$

Because all the different quantities in Equation 15 are known or measurable, we could, in principle, determine the function  $C(\Delta S)$ . Unfortunately, it is not possible to solve Equation 15 for  $c(t)$  analytically. Therefore, the concentrations must be determined numerically.

### Phantom Experiments

To check the mathematical relationship between signal intensity and gadolinium concentration, phantom measurements were performed. A total of 15 sample tubes containing human serum with different concentrations of gadopentetate dimeglumine were studied at 38°C. All measurements were performed with the same fast low-angle shot sequence parameters, which were also used for the in vivo investigations (see below). The test tubes were measured successively without any adjustment of the scanner between measurements. Figure 1 shows that the experimental results are well described by Equation 11 for concentrations up to 1 to 2 mmol. The discrepancies between data points and the theoretical curve for higher

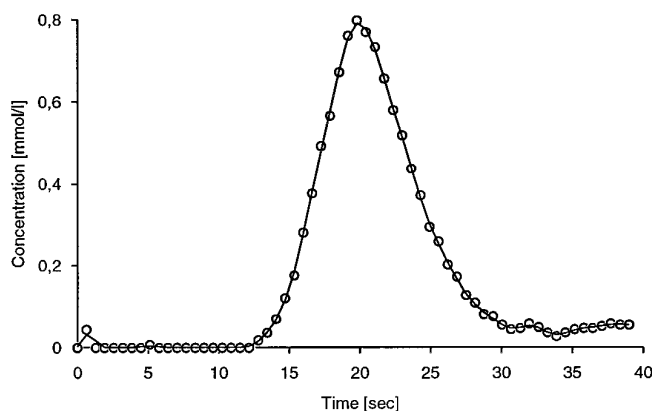


Fig 2. Time dependence of the concentration (mmol/L; commas indicate decimal places) of the contrast agent in the sagittal sinus of a healthy volunteer.

concentrations may be due to the fact that Equation 11 is based on a refocused transverse magnetization. Since no refocusing gradient was applied, the solid line overestimates the signal that was actually measured. The deviation for high concentrations above 10 mmol can be explained by macroscopic susceptibility effects.

#### Patients' Examinations

All measurements were carried out in a whole-body MR imaging/MR spectroscopy system operating at 1.5 T. A standard unspoiled fast low-angle shot sequence was used with phase-alternating radio frequency pulses and the following parameters: 6.5/3 (repetition time/echo time), flip angle of 15°, section thickness of 10 mm, matrix size of 96 × 128, and rectangular field of view of 192 × 256 mm. The k-space was sampled with a linear, nonreordered, phase-encoding scheme. To suppress flow artifacts, a nonselective 180° pulse was applied 15 milliseconds before acquisition. Experiments were performed with the same parameter settings used for the phantom investigations. Up to 64 images of a transverse section were recorded continuously with no waiting times between single images. The total measurement time for one image was 639 milliseconds.

After informed consent was obtained from the patient, solutions of 1 mmol of gadopentetate dimeglumine diluted in 10 mL NaCl were injected within 1 second into the cephalic vein via a disposable 18-gauge in-dwelling canula.

The image data were transferred via a picture archiving and communication system network to an Apple Macintosh IIx and processed with a self-designed software package. Beginning with  $N$  acquired dynamic images, the parameter images of the rCBV percentage were calculated pixel by pixel using Equation 10. Different regions of interest were also evaluated. The pixels enclosed were arithmetically averaged before the actual calculation. Measurements with the maximum number of acquisitions showed that there was no detectable recirculation of the

contrast agent (Fig 2). In some cases, the concentration-time curve leveled off after the maximum value and never reached the baseline. The main reason for this behavior was that the intravenously injected bolus dispersed upon arrival in the brain. Because the measuring time was limited and in some cases not long enough to register the complete bolus transit through the brain, the corresponding concentration-time curves did not decay completely to zero. In the case of a damaged blood-brain barrier, leakage of the contrast material into the extravascular compartment can occur and lead to the observed deviations. These effects were corrected for after integration by subtracting the area:

$$18) \quad \frac{1}{2} \cdot (t_{\text{end}} - t_{\text{peak}}) \cdot c(t_{\text{end}})$$

where  $t_{\text{end}}$  denotes the time at the end of acquisition,  $t_{\text{peak}}$  the time at which the concentration reaches its maximum, and  $c(t_{\text{end}})$  the actual concentration value at the end of acquisition.

## Results

### Normal Values

To test the validity of our method, we examined a group of 62 patients with different pathologic findings. In all cases the various diseases were confined within one hemisphere of the brain. To determine normal values of the mean CBV, we selected a region of interest on the calculated rCBV images that completely encompassed the contralateral healthy hemisphere. For the CBV we found a mean value of  $4.6 \pm 1.6$  vol%, which is in good accordance with reference values (see the Table).

### Case Studies

**Case 1.**—A 76-year-old patient with progressively worse headache was examined. MR im-

Cerebral blood volume values for healthy brain tissue

Study	Imaging Method	No. of Examinations	Cerebral Blood Volume, vol%
Current	MR imaging	62	$4.6 \pm 1.6$
Grubb et al (29)	Emission tomography	10	$4.3 \pm 0.5$
Inoue et al (37)	Single-photon emission computed tomography	10	$4.1 \pm 0.6$
Sabatini et al (38)	Single-photon emission computed tomography	9	$3.4 \pm 0.3$
Rempp et al (7)	MR imaging	12	$6.9 \pm 2.2$

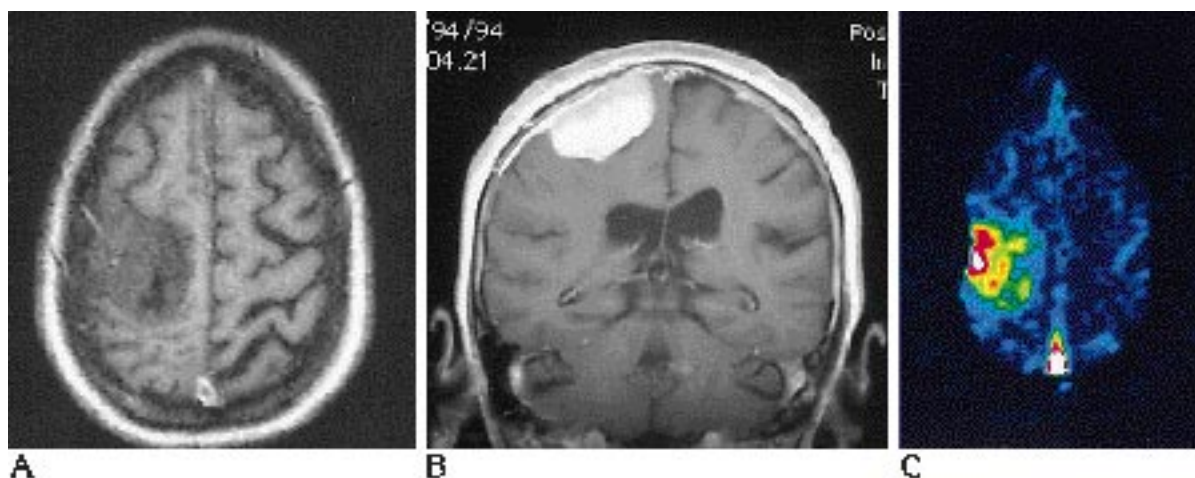


Fig 3. MR studies in a 76-year-old patient with a meningioma of the right parietal region.

A, Initial T1-weighted MR image.

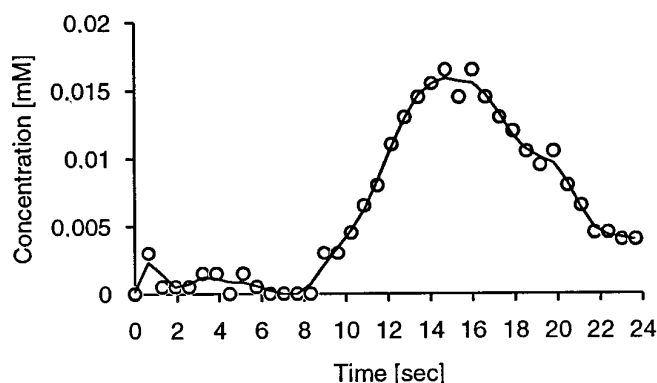
B, Contrast-enhanced coronal view.

C, Axial MR image with a color scale ranging from 0 to 48 vol% cerebral blood volume per pixel.

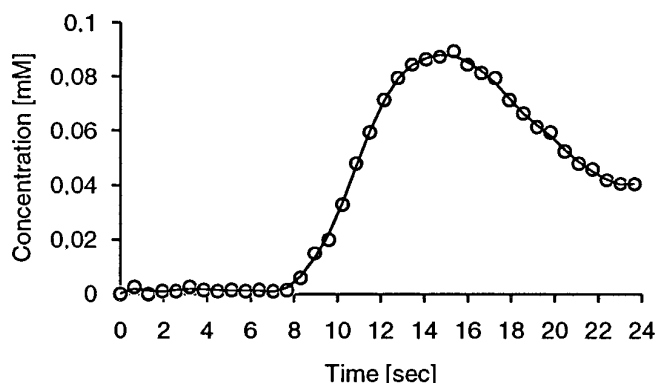
aging revealed a parietal tumor with an internal structure. Different signal intensities were observed in the initial measurement series followed by a strong enhancement in the area of the tumor after administration of contrast agent (Fig 3). The diagnosis of a meningioma was later confirmed histologically. For the intact left hemisphere, the median blood volume was estimated from the MR image and found to be 4.4%, whereas for the lateral portions of the tumor a value of 39% was found. In addition, three representative regions of interest located within the gray matter of the intact hemisphere, within the tumorous tissue, and within the sagittal sinus were examined. The results are plotted in Figure 4. Signal intensity before the arrival of the contrast bolus was approximately 30 (in arbitrary units) for each region of interest. The maximum values for the intensities in gray matter, tumor, and sagittal sinus were 50, 130, and 260, respectively. The corresponding concentration-time curves are in good agreement with typical results of conventional nuclear medicine investigations. The delay of 2 seconds between the arrival of the bolus in the sagittal sinus and its arrival in the gray matter corresponds to the expected value for the transit time through the capillaries. There was no return to baseline values after the first pass in this patient, possibly because of the damaged blood-brain barrier in the meningioma, which

allowed leakage of contrast agent and thus led to difficulties in determining the *absolute* value for rCBV. We corrected for this baseline offset by introducing Equation 18 before calculating the rCBV values.

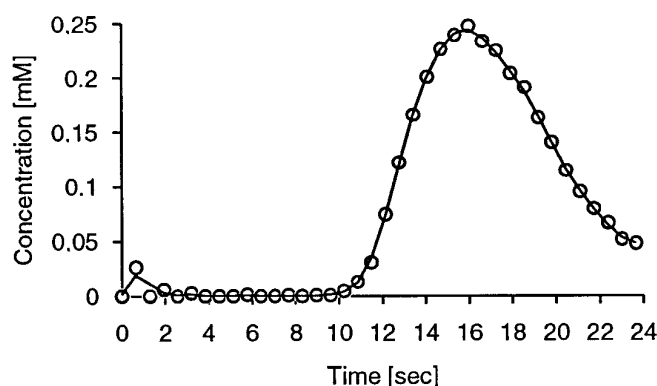
**Case 2.**—A 66-year-old patient was admitted with paresis of the left foot and typical stroke symptoms. Eight hours after the symptoms appeared the patient was examined for the first time by MR imaging. The initial morphologic images showed no striking anomalies (Fig 5A). After administration of heparin, the symptoms vanished almost completely during the following days. Four days after the first event, paresis developed on the left side, along with an obvious cognitive disorder. MR imaging, including rCBV measurements, was performed 4 hours after the onset of symptoms. The T2-weighted image showed a new area of signal enhancement within the right cerebral cortex (Fig 5C). The signal pattern corresponded closely to that of a stroke that had occurred only a few hours earlier within the area supplied by the right middle cerebral artery. An analysis of the two sets of measurements, which were both performed during the acute phase of the ischemia, provided further information. The blood volume map recorded after the first event revealed reduced perfusion within the right precentral region (Fig 5B). Normalization of perfusion in this region correlated well with improvement after



A



B



C

Fig 4. Concentration-time curves for different tissues of the patient in Figure 3. Gray matter (region of interest, 16 pixels) (A); tumor tissue (region of interest, 16 pixels) (B); sagittal sinus (region of interest, 3 pixels) (C). *mM* indicates millimoles.

the first paresis. The results of the second examination disclosed reduced perfusion in the left frontal region in addition to its reduction of up to 50% within the right central region (Fig 5D).

## Discussion

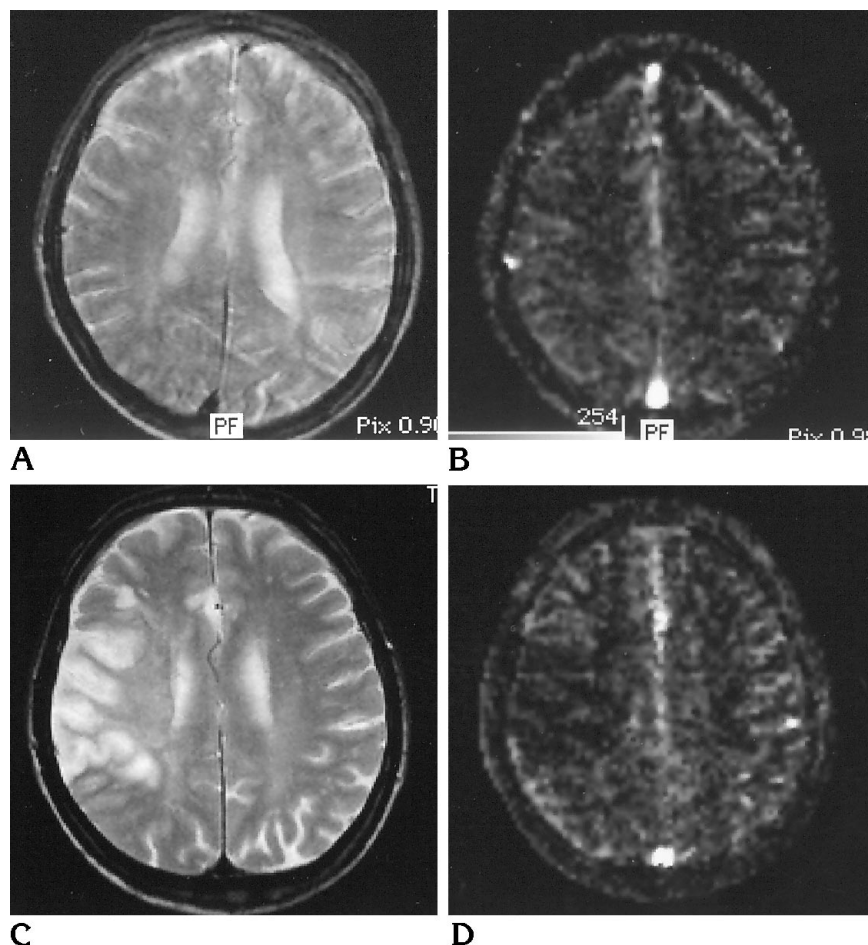
A prerequisite to the use of the indicator-dilution method for calculating perfusion parameters is the possibility of quantifying the concentration of the indicator in the tissue. This presents a problem in MR imaging, since the primary measured quantity (ie, signal intensity) is merely a number. Only by using theoretical models and performing reference measurements is it possible to quantify concentrations. The method proposed by Rosen et al (4) (ie, injecting 0.1 mmol gadopentetate dimeglumine per kilogram of body weight and subsequently measuring signal reduction caused by the susceptibility effect) has been the subject of controversial discussions (27). Another problem with this procedure results from the long echo times necessary to obtain a sufficient signal-to-noise ratio. Without the echo-planar imaging technique it takes approximately 2.2 seconds to acquire an image with a 64-pixel matrix. Thus, the achievable time resolution may be insufficient for tracking the bolus and extracting from it the corresponding blood volume parameters.

Nevertheless, using the relaxation method it is possible to establish a link between signal intensity and mean concentration of contrast agent that is based on theoretical considerations as well as on experimental knowledge of the relaxivities of the agent in human serum. Since no corresponding relaxivity values are reported by the manufacturer for gadopentetate dimeglumine at a field strength of 1.5 T, it was necessary to determine such values experimentally. Although the error is estimated to be about 10%, our measurements on phantoms containing different concentrations of gadolinium confirm the theoretically expected dependence. However, it is important to ensure that the arterial concentration of the bolus does not exceed a maximum value during intravenous administration; otherwise, no unambiguous relationship between signal intensity and concentration can be established. As already demonstrated by Hackländer et al (26), this can be accomplished by injecting 1 mmol of gadopentetate dimeglumine within 1 second. Since only about one



Fig 5. T2-weighted MR image (A) and absolute cerebral blood volume map (B) of a 66-year-old man 8 hours after first ischemic event in the supply area of the right middle cerebral artery.

C and D, Corresponding follow-up studies 4 days later, 4 hours after the second stroke.



eighth of the normally administered amount of contrast agent is used for one perfusion study, multiple dosing (eg, for different section positions) is possible without exceeding the total allowable amount of agent.

We have shown that the agent can be used as an indicator for the entire intravascular compartment (ie, for plasma as well as for corpuscular volume). In intact brain tissue, gadopentetate dimeglumine can be regarded as an intravascular contrast agent because it does not pass the intact blood-brain barrier. This remains also true to first order (ie, first approximation) if the blood-brain barrier is damaged by a pathologic process, since diffusion times are normally long compared with the passage time of the bolus. However, as our first case study indicates, this statement is not necessarily valid for tumors in which there is a severely damaged blood-brain barrier. In tumors such as meningiomas, the diffusion times of the contrast agent

can be short enough to lead to leakage during bolus transit (18). Owing to the fact that there is no truly intravascular MR contrast agent currently available for humans, the problem of leakage has to be taken into account mathematically. Even if the quoted numbers for rCBV obtained in such cases do not represent *exact absolute* values, we can nevertheless monitor *relative* changes quite precisely. Since the rCBV images reflect only those parts of the tissue that are still being perfused, and thus that are most likely still vital, they can be used for delimiting possible locations for excision of brain tumors.

We found a CBV of  $4.6 \pm 1.6$  vol% (mean of 62 subjects) for intact brain tissue, which is in good agreement with results from nuclear examinations. The corresponding mean value obtained by using the susceptibility effect yielded a value of 6.9 vol%, which represents an overestimate of about 50% (8). This discrepancy may be due to the inherent difficulties in deter-

mining parameters by using the susceptibility effect.

To describe rCBV in percentages may seem quite unusual, since the results of integral measurements of parameters of the whole brain or even of a selected section are normally given in units of milliliters per 100 g brain tissue. With increasing spatial resolution, however, it seems useful to present rCBV data as volume fractions of the total volume. This practice has also been presented in recent reports of PET studies (28). To convert both quantities, the mean density of brain tissue must be taken into account (29):

$$19) \quad rCBV \left[ \frac{\text{mL}}{100\text{g}} \right] = \frac{rCBV\%}{1.08 \frac{\text{g}}{\text{mL}}}$$

Another possible clinical application is in the early recognition of brain infarcts. Our second case study showed that a reduced CBV can be detected during the first few hours after the onset of clinical symptoms. This result is in accordance with studies done with PET, single-photon emission computed tomography, and MR tomography. They show that during the first 3 to 4 hours after reperfusion the CBV values do not change (30). During the next 20 hours the CBV decreases (31, 32), possibly because of swelling of endothelial microvilli or brain edema (33). It is only during the following days that the reduced flow, which cannot be measured by our method, can be compensated by an increased blood volume (2, 3, 34–36). Since quantitation of CBV by means of our method is performed on an absolute scale, follow-up studies during therapy are possible. This was shown in one case (see "Results") in which an area of initially reduced rCBV normalized during the next days.

To examine the pathophysiological changes within an infarct region in more detail, it would be desirable to know more about dynamic aspects, such as, for example, blood flow. This, however, requires information about the functional status of arterial input, which cannot be directly deduced from measured data. Work in this direction is in progress. Currently, the method presented here is being applied to patients in our department to test its reliability on a much broader data set. Since it extends examination times only by a few minutes, it is applicable in routine clinical settings.

The method yields results with higher spatial resolution than other (eg, nuclear medicine) methods.

In summary, a method is available that allows measurements of rCBV even with conventional clinical MR scanners without echo-planar imaging capability.

## Acknowledgment

We thank C. Stasch for technical assistance.

## References

1. Aronen HJ, Gazit IE, Louis DN, et al. Cerebral blood volume maps of gliomas: comparison with tumor grade and histologic findings. *Radiology* 1994;191:41–51
2. Heiss WD, Herholz K. Assessment of pathophysiology of stroke by positron emission tomography. *Eur J Nucl Med* 1994;21:455–465
3. Reiche W, Weiller C, Isensee C, et al. Verlaufsuntersuchungen mit Fluß/Volumen-(F/V-)SPECT und MRT/CT bei Patienten mit striatokapsulären Infarkten. *Klin Neuroradiol* 1993;3:78–84
4. Rosen BR, Belliveau JW, Veraa JM, Brady TJ. Perfusion imaging with NMR contrast agents. *Magn Reson Med* 1990;14:249–265
5. Belliveau JW, Kennedy DN, McKinstry RC, et al. Functional mapping of the human visual cortex by magnetic resonance imaging. *Science* 1991;254:716–719
6. Gückel F, Rempp K, Becker G, Köpke J, Loose R, Brix G. Kernspintomographie als funktionsdiagnostische Methode. *Radiologe* 1994;34:619–626
7. Rempp K, Brix G, Wenz F, Becker CR, Gückel F, Lorentz WJ. Quantification of regional cerebral blood flow and volume with dynamic susceptibility contrast-enhanced MR imaging. *Radiology* 1994;193:637–641
8. Gückel F, Brix G, Rempp K, Deimling M, Röther J, Georgi M. Assessment of cerebral blood volume with dynamic susceptibility contrast enhanced gradient-echo imaging. *J Comput Assist Tomogr* 1994;18:344–351
9. Dean BL, Lee C, Kirsch JE, et al. Cerebral hemodynamics and cerebral blood volume: MR assessment using gadolinium contrast agent and T1-weighted turbo-FLASH imaging. *AJNR Am J Neuroradiol* 1992;13:39–42
10. Zierler KL. Theoretical basis of indicator-dilution methods for measuring flow and volume. *Circ Res* 1962;10:393–407
11. Lassen NA, Perl W. Volume/flow or mass/flux ratio (mean transit time): bolus injection. In: *Tracer Kinetic Methods in Medical Physiology*. New York, NY: Raven, 1979:76–101
12. Grodins FS. Basic concepts in the determination of vascular volumes by indicator-dilution methods. *Circ Res* 1962;10:429–446
13. Zierler KL. Equations for measuring blood flow by external monitoring of radioisotopes. *Circ Res* 1965;16:309–321
14. Weisskoff RM, Chesler D, Boxerman JL, Rosen BR. Pitfalls in MR measurement of tissue blood flow with intravascular tracers: which mean transit time? *Magn Reson Med* 1993;29:553–559
15. Bloembergen NJ. Proton relaxation times in paramagnetic solutions. *J Chem Phys* 1957;27:572–573
16. Solomon I. Relaxation processes in a system of two spins. *Physiol Rev* 1955;99:559–565
17. Albert MS, Huang W, Lee JH, Balschi JA, Springer CS. Aqueous shift reagents for high-resolution cation NMR VI. *NMR Biomed* 1993;6:7–20

18. Gowland P, Mansfield P, Bullock P, Stehling M, Worthington B, Firth J. Dynamic studies of gadolinium uptake in brain tumors using inversion-recovery echo-planar imaging. *Magn Reson Med* 1992;26:241-258
19. Pykett IL, Rzedzian RR. Instant images of the body by magnetic resonance. *Magn Reson Med* 1987;5:563
20. Mansfield P. Multi-planar image formations using NMR spin echoes. *J Phys C: Solid State Phys* 1977;10:L55-L58
21. Haase A. Snapshot FLASH MRI: applications to T1, T2 and chemical-shift imaging. *Magn Reson Med* 1990;13:77-89
22. Hänicke W, Merboldt KD, Chien D, Gyngell ML, Bruhn H, Frahm J. Signal strength in subsecond FLASH magnetic resonance imaging: the dynamic approach to steady state. *Med Phys* 1990;17:1004-1010
23. Zur Y, Stokar S, Bendel P. An Analysis of fast imaging sequences with steady-state transverse magnetization refocusing. *Magn Reson Med* 1988;6:175-193
24. Frahm J, Merboldt KD, Hänicke W, Haase A. Flow suppression in rapid FLASH NMR images. *Magn Reson Med* 1987;4:372-377
25. Hackländer T. Parameterbilder des cerebralen Blutvolumens mit T1 gewichteten FLASH Sequenzen. *Röntgenpraxis* 1995;48:146-152
26. Hackländer T, Hofer M, Paselk C, Mödder U. Funktionelle Bildgebung des Gehirns mit niedrig dosiertem Gadolinium DTPA und Turbo-FLASH Sequenzen. *Rofo Fortschr Geb Rontgenstr Neuen Bildgeb Verfahr* 1993;158,4:348-354
27. Kennan RP, Zhong J, Gore JC. Intravascular susceptibility contrast mechanisms in tissue. *Magn Reson Med* 1994;31:9-21
28. Leenders KL, Perani D, Lammertsma AA, et al. Cerebral blood flow, blood volume and oxygen utilization: normal values and effect of age. *Brain* 1990;113:27-47
29. Grubb RL, Raichle ME, Higgins CS, Eichling JO. Measurement of regional cerebral blood volume by emission tomography. *Ann Neurol* 1978;4:322-328
30. Pappata S, Fiorelli M, Rommel T, et al. PET study of changes in local brain hemodynamics and oxygen metabolism after unilateral middle cerebral artery occlusion in baboons. *J Cereb Blood Flow Metab* 1993;13:416-424
31. Heiss WD, Graf R, Wienhard K, et al. Dynamic penumbra demonstration by sequential multitracer PET after middle cerebral artery occlusion in cats. *J Cereb Blood Flow Metab* 1994;14:892-902
32. Maeda M, Itoh S, Ide H, et al. Acute stroke in cats: comparison of dynamic susceptibility-contrast MR imaging with T2- and diffusion-weighted MR imaging. *Radiology* 1993;189:227-232
33. Kuschinsky W, Paulson OB. Capillary circulation in the brain. *Cerebrovasc Brain Metab Rev* 1992;4:262-286
34. Buell U, Braun H, Ferbert A, Stiner H, Weiller C, Ringelstein EB. Combined SPECT imaging of regional cerebral blood flow (99mTc-hex-amethyl-propyleneamine oxime, HMPAO) and blood volume (99mTc-RBC) to assess regional cerebral perfusion reserve in patients with cerebrovascular disease. *Nucl Med* 1988;27:51-56
35. Gjedde A, Kuwabara H, Hakim AM. Reduction of functional capillary density in human brain after stroke. *J Cereb Blood Flow Metab* 1990;10:317-326
36. Weiller C, Ringelstein EB, Reiche W, Thron A, Buell U. The large striatocapsular infarct. *Arch Neurol* 1990;47:1085-1091
37. Inoue Y, Momose T, Machida K, et al. Quantitation of cerebral blood volume by 99mTc-DTPA-HSA SPECT. *Radiat Med* 1992;10:184-188
38. Sabatini U, Celsis P, Viallard G, Rascol A, Marc-Vergnes JP. Quantitative assessment of cerebral blood volume by single-photon emission computed tomography. *Stroke* 1991;22:324-330

Please see the Commentary on page 841 in this issue.